Influence of structure characteristics on wave transmission and shoreline response at a low-crested segmented breakwater in Little Egg Harbor Township, NJ

By

Katherine M. Gannon, Matthew S. Janssen, and Jon K. Miller
Davidson Laboratory, Stevens Institute of Technology, Hoboken, NJ 07030; kgannon@stevens.edu

ABSTRACT

Graveling Point Beach, a public beach within Little Egg Harbor Township, New Jersey, has been experiencing long-term erosion. To address the issue, a living shoreline project consisting of four low-crested rubble-mound breakwaters and a beach nourishment was constructed beginning in fall 2022 (structures) and finishing in spring 2023 (beach nourishment). A variety of field methods were used to investigate the influence of the breakwater system on wave transmission and beach fill evolution. The observations are then compared to common empirical estimations. A median wave transmission coefficient of 0.4 was measured for incident waves with a median height and peak period of 9 cm and 2 sec, respectively. The observed transmission coefficient was higher than that predicted by models such as Briganti *et al.* (2003) and Van der Meer and Daemen (1994) suggesting other processes such as diffraction may be influencing the results. Structure from Motion (SfM) was used to generate a series of Digital Elevation Models (DEMs) which show salients forming behind the structures. The resulting salient growth was compared to the model of Suh and Dalrymple (1987), which was shown to overpredict the amplitude of the salient at Graveling Point. However, the expected relationship of breakwaters with increased offshore distance having shorter salient lengths was generally observed. The equation was refit using the field data at Graveling Point and laboratory data with similar wave heights and periods from Suh and Dalrymple to derive a modified model that may be more appropriate in low-energy environments.

KEYWORDS: Living shoreline, low-crested breakwater, wave transmission, wave diffraction, salient.

Manuscript submitted 27 May 2024; revised and accepted 4 July 2024.

Graveling Point Beach is a public beach in Little Egg Harbor Township, New Jersey, that provides upland protection to the community from storm events and recreational opportunities for residents (Figure 1). The site has been subject to long-term erosion. In 2020, a local architecture and engineering firm was contracted by the township to design a living shoreline project that would both widen the beach and address the ongoing erosion. The final design consisted of a beach nourishment, four low-crested shore parallel stone breakwaters, and a stone groin (U.S. Army Corps of Engineers Philadelphia District 2021). The construction was completed in phases with the stone structures constructed in fall 2022 and the nourishment in spring 2023 (Figure 2). In this study, the definition of low-crested is consistent with that used by Van der Meer and Daemen (1994) and Briganti *et al.* (2003). Those studies use "low-crested" to refer to structures where the ratio of freeboard to incident wave height is less than five or when the ratio of freeboard to median stone size is less than two.

Several unique features of the project provided an opportunity to gain a greater understanding of the wave-attenuating impacts of the breakwater system on shoreline morphology in the months following a nourishment event. The shoreline's limited extent (approximately 300 m long), the presence of a groin downdrift, and a limited fetch of approximately 7 km create a set of relatively controlled conditions (Kerr *et al.* 2020) that allows for a finer scale analysis of the beach fill evolution. Further, one of the breakwaters was constructed with a visible offset in elevation (marked with a star in Figure 2; Figure 3) providing a unique opportunity to compare the effect of crest height on wave transmission. The halves of the breakwater being compared are referred to as "taller" and "shorter." It was hypothesized that shoreline development behind this breakwater would be sensitive to this difference in transmission since the fill was uniformly placed without varying the alongshore density.

It is hoped that the results of the present study can improve the understanding of wave transmission over, around, and through low-crested segmented structures and that this information can be used to improve future designs. Similarly, it is hoped that the measured morphological changes can be used to improve formulas for predicting the response of shorelines to low-crested segmented breakwaters in low-moderate energy settings.

BACKGROUND

Wave transmission

When waves interact with a set of low-crested breakwaters such as that shown in Figure 2, a portion of the energy will be reflected, a portion will be dissipated, and a portion will be transmitted. Wave gauges placed offshore of the structure will predominantly measure the incident wave energy (reflection is assumed small). Wave gauges placed behind the structure will record the transmitted energy, but also a portion of the energy of the waves passing through the gaps (diffraction).

Wave transmission is typically quantified by comparing the ratio of the transmitted (inshore) wave height (H_t) to the incident (offshore) wave height (H_i) to calculate a wave transmission coefficient (K_t) (Equation 1).

$$K_t = H_t/H_i \quad (1)$$

In such calculations, it is generally assumed that the amount of energy transmitted around the structure is negligible.

Figure 1 (left). Graveling Point's (marked by star) maximum fetch in Great Bay. Photo from ArcGIS software by Esri for MAXAR satellite imagery and world ocean layer.

K_t decreases as the amount of transmitted wave energy decreases. Empirical studies have identified several structure characteristics that influence the amount of wave height reduction that is achieved, including: crest height (h_s), crest width (B), structure slope (m), and median stone diameter (D_{50}). More specifically, the height of the crest above the water level (d) plays an important role in determining the amount of wave transmission that occurs via overtopping. The height of the crest above the water level is known as the freeboard (R_c).

The characteristics of the wave climate also play a role in the amount of wave transmission that occurs. For example, wave steepness (S_{op}) can be calculated by measuring the peak period (T_p) correlated to the incident waves (Equation 2) which then informs the surf similarity parameter (ξ) (Equation 3). Note that the use of the incident wave height at the toe of the structure (Van der Meer and Daemen 1994; Briganti *et al.* 2003) varies from the typical use of deep-water wave height (g is gravitational acceleration):

$$S_{op} = 2\pi H_i / g T_p^{\,2} \qquad (2)$$

$$\xi = m/\sqrt{S_{op}} \qquad (3)$$

For empirical models that predict wave transmission, crest elevation is critical for breakwater design because small changes can lead to significant differences in wave transmission (Chasten *et al.* 1993). Crest width also influences the amount of wave energy that is transmitted through overtopping along the crest of the structure; wider crest widths lead to lower amounts of energy transmitted inshore (Briganti *et al.* 2003). Hassanpour *et al.* (2023) determined from laboratory testing of low-crested breakwaters and a comprehensive review of existing wave transmission formulas that the Van der

Figure 2 (left). Graveling Point Beach, Little Egg Harbor Township, New Jersey, before (March 8) and after (April 17) the nourishment that occurred in late March 2023. The breakwater starred in the figure was the subject of the wave study. Photo from ArcGIS software by Esri for MAXAR satellite imagery.

Figure 3. Breakwater constructed with offset at Graveling Point Beach.

Meer and Daemen (1994), Briganti *et al.* (2003), and d'Angremond *et al.* (1996) formulas had the lowest root mean squared error. The tested ranges of parameter values over which the empirical equations were derived are given.

The Van der Meer and Daemen equation suggests that wave transmission is linearly related to non-dimensional freeboard, as given by Equation 4 where D_{50} is used as the non-dimensionalizing parameter. In the equation, the slope term is related to a non-dimensionalized incident wave height, while the intercept is related to both non-dimensionalized wave height and crest width.

$$K_t = a\,(R_c/D_{50}) + b \quad (4)$$

Where $a = 0.031\,(H_i/D_{50}) - 0.24$ and $b = 5.42S_{op} + 0.0323\,(H_i/D_{50}) - 0.0017\,(B/D_{50})^{1.84} + 0.51$

Tested range limitations: $-2 < R_c/D_{50} < 2$; $1 < H_i/D_{50} < 6$; $0.01 < S_{op} < 0.05$

In the Briganti *et al.* and d'Angremond *et al.* formulas, wave transmission is given as a function of non-dimensional freeboard (R_c/H_i) and crest width (B/H_i). For narrow crested structures ($B/H_i < 10$), Briganti *et al.* and d'Angremond *et al.* are the same equation; however, Briganti *et al.* expanded the testing ranges for relative freeboard and crest widths. The Briganti *et al.* equation is given by Equation 5 and is used as a benchmark against which the observed values could be compared.

For $B/H_i > 10$: (5)

$$K_t = -0.35\,(R_c/H_i) + 0.51\,(B/H_i)^{-0.65}\,(1 - e^{(-0.41\xi)})$$

For $B/H_i < 10$: (5)

$$K_t = -0.4\,(R_c/H_i) + 0.64\,(B/H_i)^{-0.31}\,(1 - e^{(-0.5\xi)})$$

Tested range limitations: $-5.0 < R_c/H_i < 5.0$; $0.37 < B/H_i < 102.12$; $0.002 < S_{op} < 0.07$

Table 1 and Figure 4 provide a summary of the parameters included in most empirical wave transmission formulations and how they were measured. In the present study, crest width, breakwater slope, and median stone size are all fairly consistent along the length of the breakwater in question. This isolates the influence of the varied crest height between the two sides of the breakwater and the freeboard which varies with each collected burst of data. Additional details for the measured parameters are provided in the Field Methods section.

Wave diffraction

In a segmented breakwater system, the gaps between breakwaters introduce a source of diffracted wave energy which contributes to the measured inshore wave heights. Diffraction patterns are influenced by the directional spreading of incoming waves, their angle of approach relative to the gap, and the wavelength of the waves in comparison to the gap width. The amount of diffracted wave energy at a given point depends on the horizontal and vertical displacement of the point compared to the source of the diffracted energy. Wind waves locally generated have greater directional spreading than swell waves that were generated further away (Coastal Engineering Research Center [CERC] 1984). The diffraction diagrams in the Shore Protection Manual (CERC 1984) can be used to predict wave

Table 1.
Graveling Point breakwater design parameters for transmission prediction.

Parameter	Symbol	Value	Source
Crest height	h_s	Taller – 0.98 m NAVD 88; Shorter – 0.88 m NAVD 88	RTK GPS
Water level	d	Offshore mean value for each hourly, 17.1-minute burst (m NAVD 88)	RBR
Freeboard	R_c	h_s - d for each 17.1-minute burst (m NAVD 88)	See above
Peak period	T_p	Offshore peak value for each hourly, 17.1-minute burst (s)	RBR
Crest width	B	1.22 m	Design plans
Breakwater slope	m	0.67	Design plans
Median stone size	D_{50}	0.61 m	Field estimate

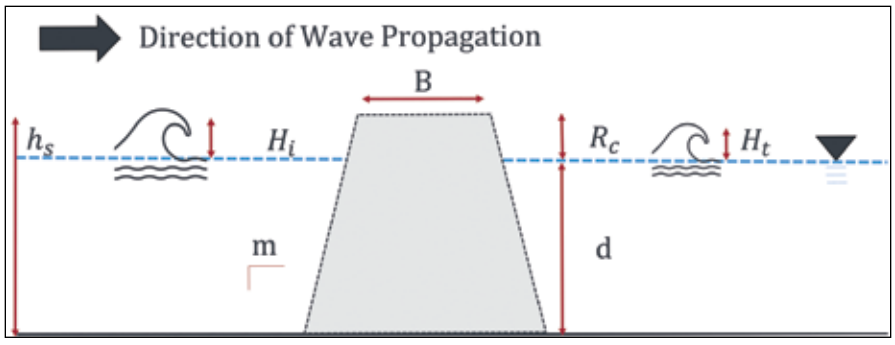

Figure 4. Schematic of how wave transmission parameters from literature are defined in this report. All parameters are measured in reference to NAVD 88 except for crest width (B).

Table 2.
Graveling Point breakwater design parameters for diffraction prediction.

Parameter	Symbol	Value	Source
Water level	d	Median value of all 720 water levels from bursts (m)	RBR
Peak period	T_p	Median value of all 720 peak periods from bursts (s)	RBR
Gap length	G	32.6 m	Design plans

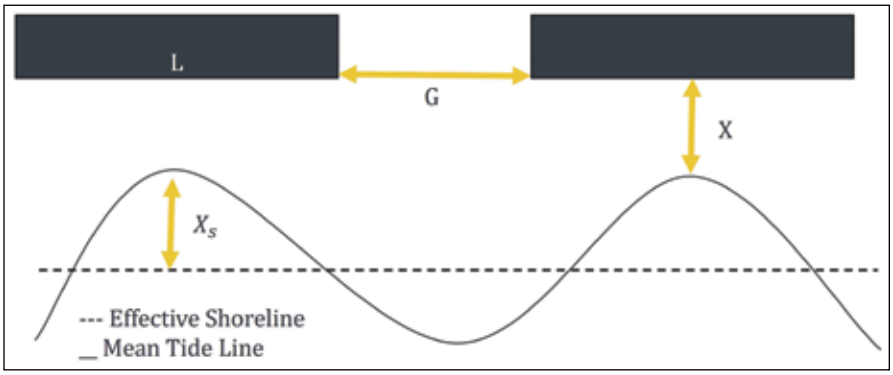

Figure 5. Schematic of how salient parameters from literature are defined in this report.

Table 3.
Graveling Point breakwater design parameters for salient development (Xs) prediction.

Parameter	Symbol	Value	Source
Gap length	G	32.6 m	Design plans
Breakwater length	L	31.4 m	Design plans
Offshore distance	X	Varies	GIS (derived from DEM)

energy patterns. Table 2 summarizes the parameters used for estimating diffracted wave heights. Here, the water level and peak period values used are the median of all bursts measured for the wave transmission study.

Shoreline response

Wave transmission and diffraction influence shoreline morphology by controlling the amount of energy allowed inshore. Sediment erodes, or scours, along the diffracted wave crest lines (Dally and Pope 1986). Behind the breakwaters, termed the shadow zone, there is low wave energy because of the diffraction pattern; this results in the accretion of sediment in that area which modifies the overall shoreline morphology (Dally and Pope 1986). The accreted sediment in the shadow zone is termed either a salient or a tombolo based on whether the accreted sediment extends to the structure once the shoreline has reached equilibrium; if the shoreline does reach the breakwater, the morphology is described as a tombolo. The apex of the salient or tombolo is typically near the center of the structure but can vary with the wave climate at the site (Dally and Pope 1986). The length of the salient or whether a tombolo is formed is dependent on the breakwater design — indirectly through limited transmission and directly through the length and placement of the breakwaters. Suh and Dalrymple (1987) used historical field data of segmented breakwater systems to determine the influence of gap width (G), distance offshore (X), and the length of the breakwater (L) on the resulting salient length behind the breakwater (X_s).

Table 3 provides a summary of the parameters considered for salient development at Graveling Point. Figure 5 illustrates how these values were measured from the Digital Elevation Models (DEMs). Suh and Dalrymple (1987) utilize the original still water shoreline before breakwater construction as the reference for measuring salient length (X_s) and offshore distance (X). Because this study began after breakwater construction, the original still water location was unknown, so instead, a reference line referred to as the effective shoreline was used which was assumed to be the halfway point between the crest and trough of the sinuous mean tide line. The distance from the effective shoreline to the crest of the salient was X_s, and the perpendicular distance from the crest of the salient to the closest point on the breakwater was X. More details are provided in the Field Methods and Shoreline Response sections for identifying the mean tide line.

FIELD METHODS

Four visits to the site for data collection occurred; the first was about two weeks after the March nourishment in April 2023, followed by May, November, and December 2023. A summary of the data collected at these visits is provided in Table 4. During each site visit, a drone survey of the beach at low tide was conducted to collect elevation data for the beach profile. It was critical to survey at low tide to ensure that all of the mean tide line was visible to the drone on the dry beach. The protocol outlined in Zimmerman *et al.* (2020) was utilized for placement of ground control points, flight parameters, and processing of the elevation data via Structure from Motion (SfM) to create a DEM) for each survey. During the initial site visit, Real-Time Kinematic GPS (RTK GPS) was utilized to measure the crest elevation of the breakwater being studied for wave transmission. The goal was to try and limit as much bias in surveying location as possible by surveying across the width of the crest at both high and low points on the stones, leading to the collection of approximately 15 survey points across each 3 m section of the approximately 31.4 m long breakwater. It was found that the average

Table 4.
Summary of data collected during site visits.

	Beach profile	Breakwater crest		Wave/water level
Date	Drone survey	RTK/GPS	Drone survey	Pressure sensors
17 April 2023	X	X	X	N/A
15 May 2023	X	N/A	N/A	N/A
6 November 2023	X	N/A	N/A	Deployed
6 December 2023	X	N/A	N/A	Retrieved

crest elevation of the structure was 0.98 m NAVD 88 (standard deviation 0.14 m) for one half of the breakwater, and 0.88 m NAVD 88 (standard deviation 0.09 m) for the other — a 10 cm difference between the two sides of the breakwater (Figure 6). A new technique was also tested for measuring the crest elevations via drone survey. Zimmerman's *et al.* (2020) methodology of using flat ground control point targets could not be applied here because of the roughness of the breakwater crest. Instead, washable orange paint was applied in X shapes to serve as the known control points. A 0.5 m long X was drawn about every 4.5 m along the length of the breakwater, centered across the width. Zimmerman *et al.*'s (2020) methodology was also modified to reduce the flight altitude from about 115.8 m to 31.4 m to optimize the resolution of the breakwater elevation. The same SfM processing was completed to develop a DEM, and the results aligned well with the RTK GPS survey with one-half of the breakwater being noticeably higher in elevation than the other (Figure 7). In November, three RBRsolo3-D wave16 high-frequency pressure sensors (RBRs) were deployed; one RBR was placed centered offshore of the breakwater of interest while the other two RBRs were placed inshore and centered on the respective halves of the breakwater ("taller" and "shorter") each approximately 7.6 m from either end of the breakwater. The inshore sensors were placed about 12.2 m from the breakwater and the offshore sensor was about 6.1 m from the breakwater (Figure 8). The sensors collected data hourly on the hour at a sampling rate of 16 Hz for 17.1-minute bursts over one month for a total of 720 bursts. From each burst, a zero-moment wave and corresponding peak period were obtained as well as an average water level. These burst sizes allowed for the variation in water levels from both the tide and storm surge to be considered. November

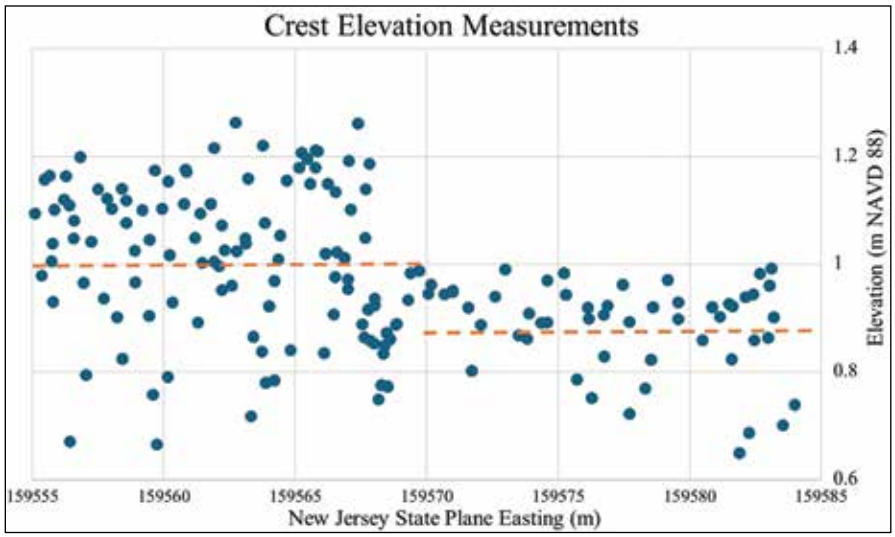

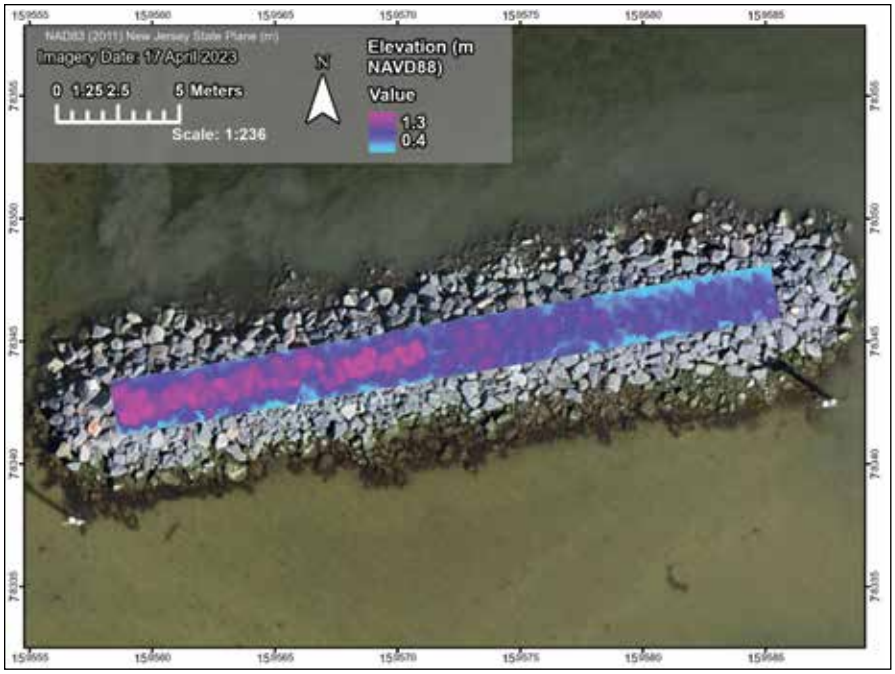

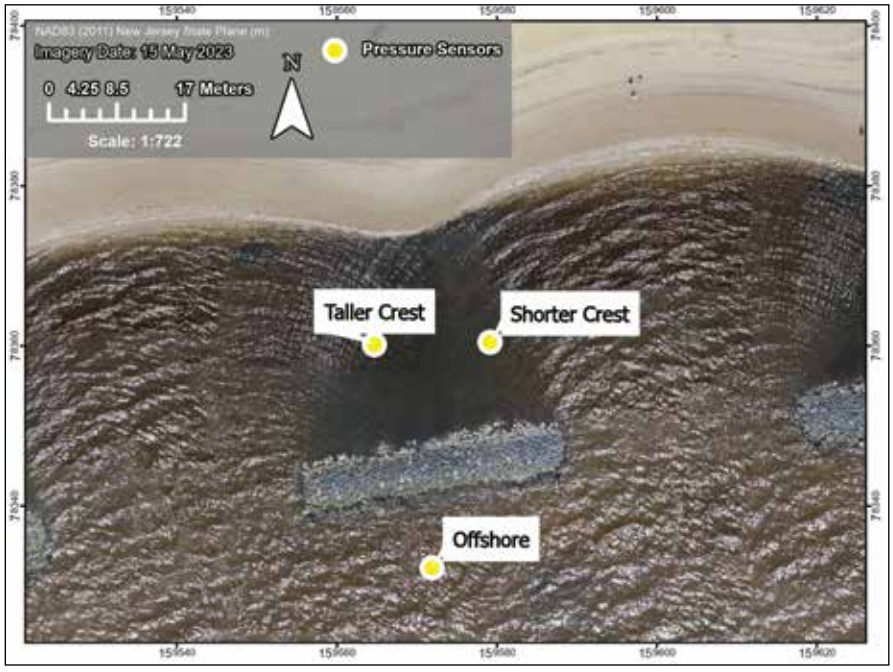

Figure 6 (top). Elevation of breakwater crest measured in m NAVD 88 via RTK GPS. Dashed lines illustrate average taller: 0.98 m and average shorter: 0.88 m elevations.

Figure 7 (middle). Elevation of breakwater crest (m NAVD 88) obtained from drone imagery.

Figure 8 (bottom). Pressure sensor placement from 6 November to 6 December 2023.

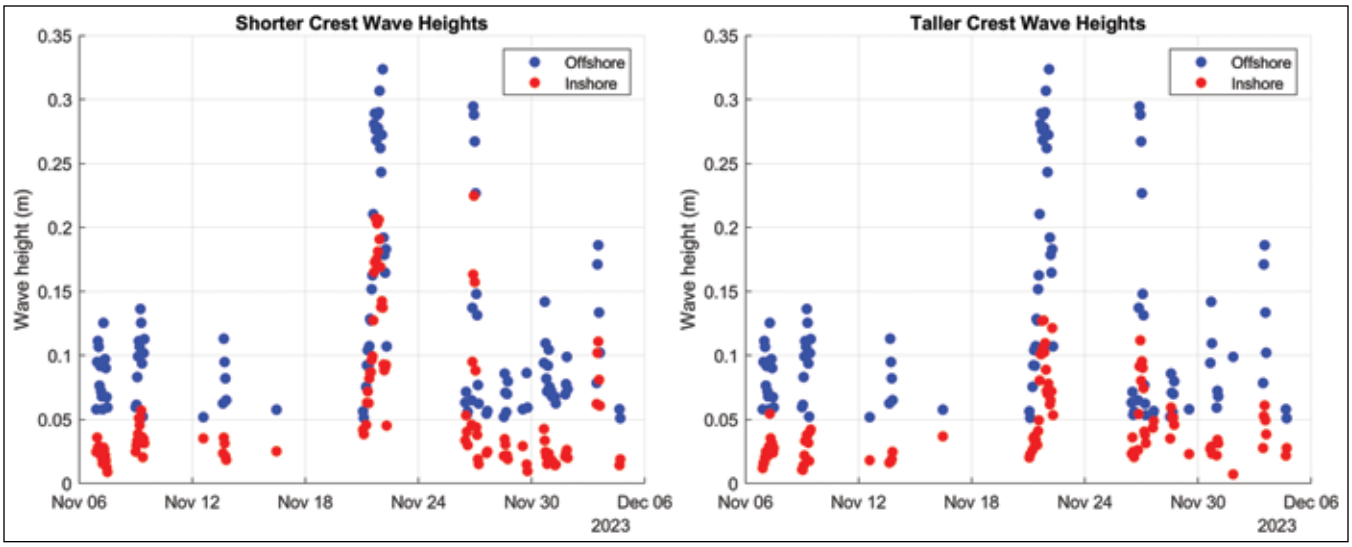

Figure 9. Offshore vs. inshore wave heights (m). Median offshore wave height = 0.09 m.

to December was selected as the wave period of study because the area typically experiences larger waves in the fall than the spring due to nor'easter activity.

RESULTS

Wave height reduction

The wave data were analyzed in the frequency domain using the MATLAB toolbox OCEANLYZ (Karimpour and Chen 2017). The peak period, zero-moment wave height, and average water level were extracted for each 17.1-minute burst. The data were then filtered to remove bursts where the peak period was less than 1.5 sec or more than 8 sec. The lower limit was the measurement threshold for the pressure gauge given the water depth, while the upper limit was a practical limit set to remove swell and other low-frequency oscillations. The data were also filtered to exclude wave heights less than 5 cm, which is considered the noise threshold for the instruments. The filtered data set is shown in Figure 9. Gaps in the data generally correspond to calm periods when the measured wave heights did not meet the height/period thresholds. Overall, wave heights were small at the site with a median offshore wave height of about 9 cm and median peak periods of approximately 2 sec.

Wave transmission coefficients were calculated for both the shorter and taller sections of the breakwater (Figure 10). The average coefficient across the shorter section was 0.41, while the average coefficient for the taller section was found to be 0.36. This suggests that the difference in crest height does not have a significant impact on wave transmission for the data set as a whole. When the data set is reexamined however, focusing only on the events where the offshore wave height is greater than 15 cm, a different picture emerges. Wave transmission coefficients for only the large events are plotted in Figure 11. When only the largest wave events are considered, the differences between the tall and short sides of the breakwater are more pronounced. During large wave events, the median transmission coefficient increases to nearly 0.60 behind the shorter section, while behind the taller section, the transmission coefficient is roughly the same as it was for the full data set (0.35 vs. 0.36). This suggests that during larger events, the shorter section is overtopped and experiences significant wave transmission, while the taller section is capable of limiting overtopping/wave transmission.

Shoreline response

Once the DEMs were developed for each survey, like the one seen for April in Figure 12, the DEMs were loaded to ArcGIS and the mean tide level elevation

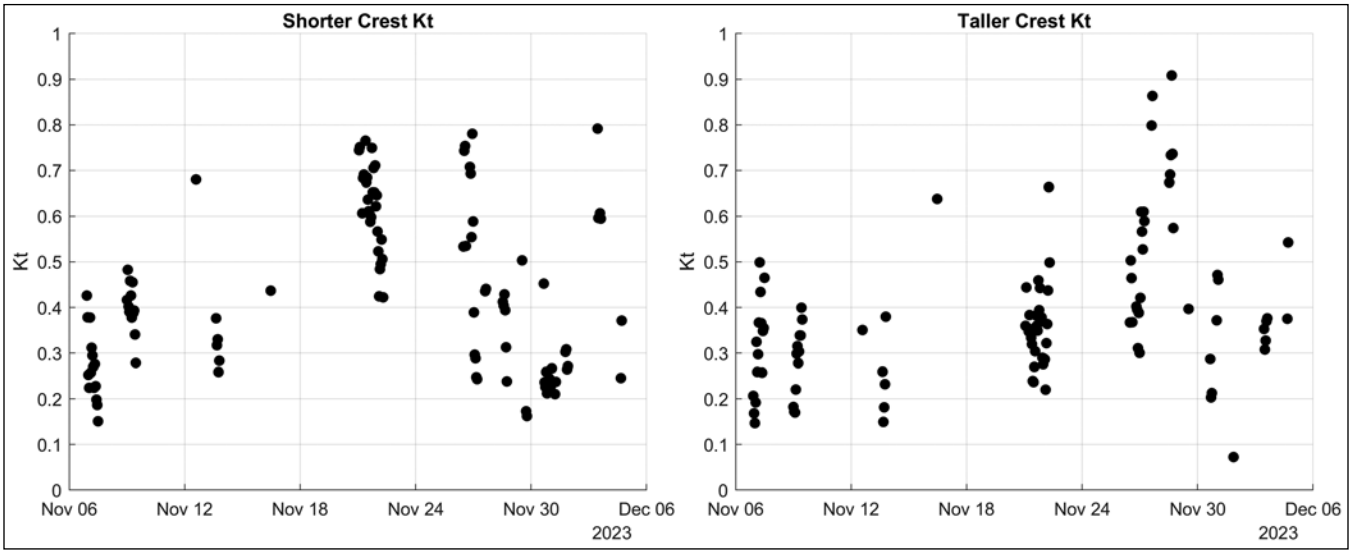

Figure 10. Observed transmission coefficients. Shorter median K_t: 0.41, taller median K_t: 0.36.

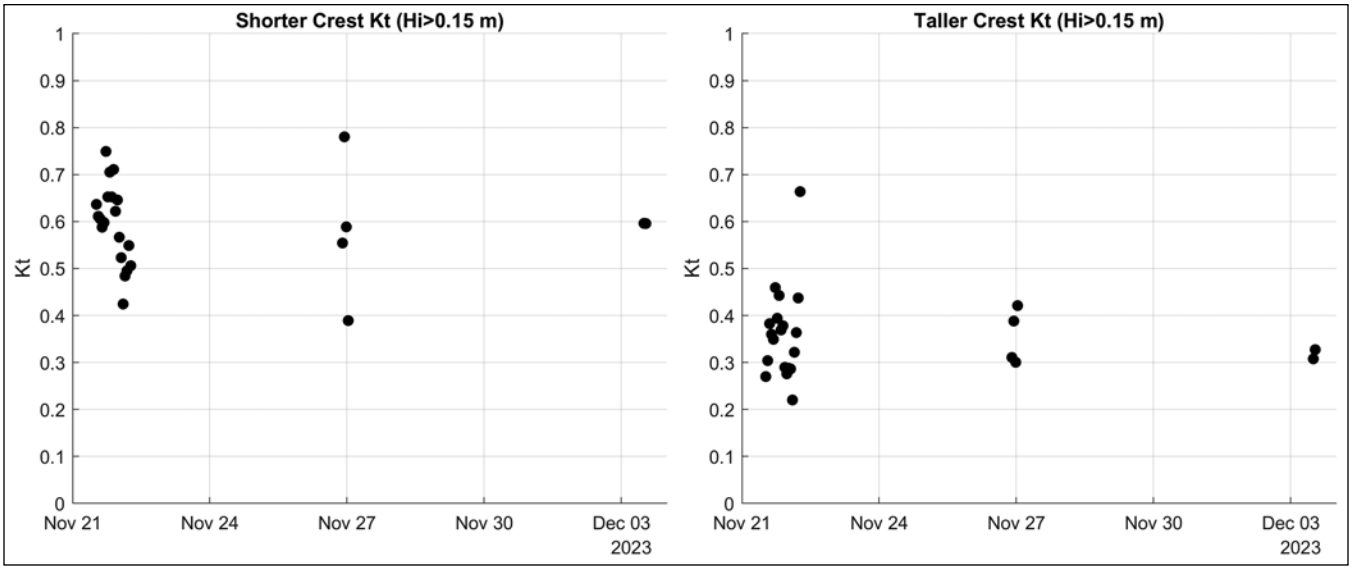

Figure 11. Observed transmission coefficients for offshore waves taller than 0.15 m. Shorter median K_t: 0.60, taller median K_t: 0.35.

of 0.0061 m NAVD 88 was tracked using the contour tool. Figure 13 shows that the mean tide level location does not change much from survey to survey, and there does not appear to be a noticeable difference in the salient apex location behind the breakwater with the offset in elevation (B) compared to the others.

The mean tide contours were then used to measure the length of the salient and the distance offshore for each of the structures during each survey as described by Figure 5. The summary of these measurements is displayed in Table 5.

For a more robust dataset, the small salients formed before the nourishment (Figure 2) behind breakwaters A and B and lack thereof behind C and D were also measured along with their corresponding distances offshore. This meant the full Graveling Point salient dataset included five salient lengths and distances offshore for each breakwater to be compared to the Suh and Dalrymple (1987) empirical method.

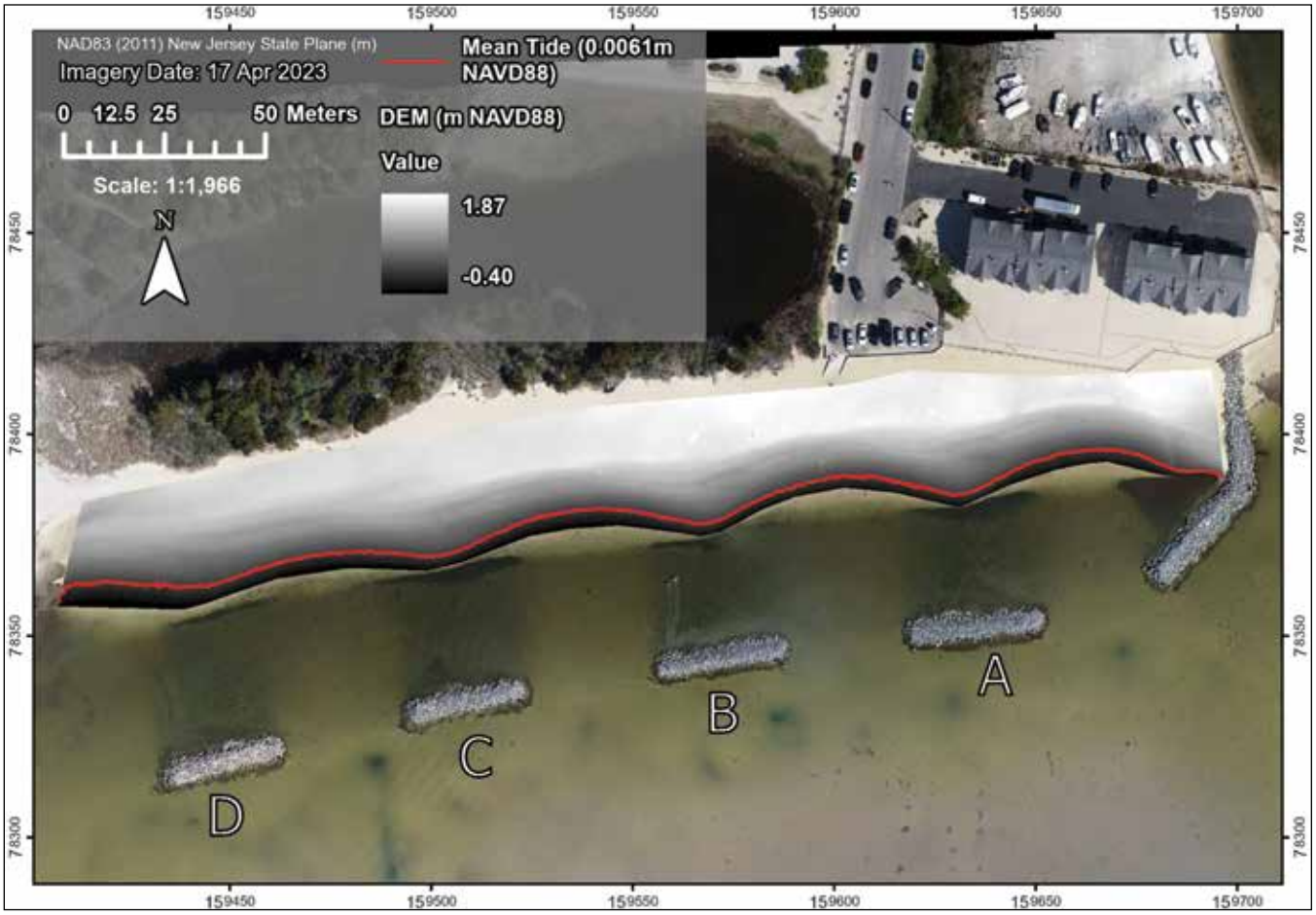

Figure 12. April 2023 Digital Elevation Model with Mean Tide Level outlined.

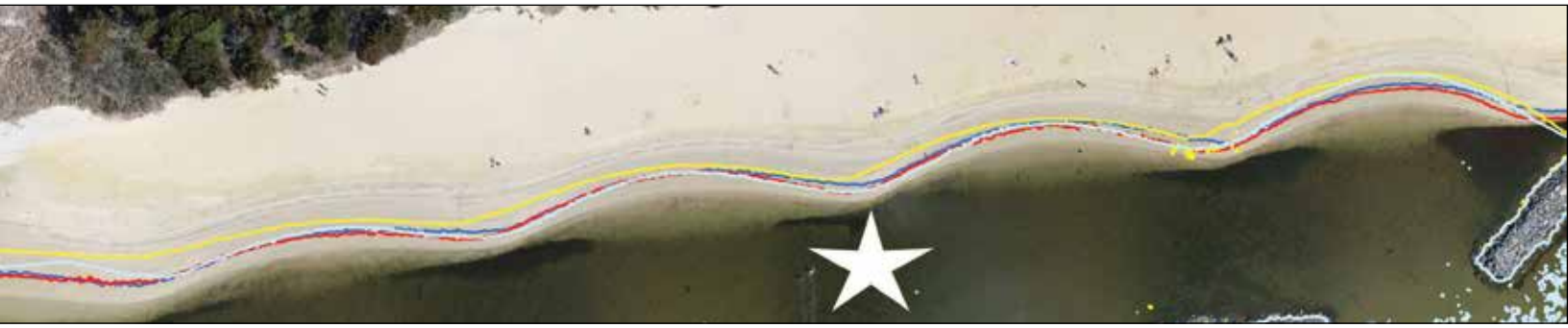

Figure 13. Mean Tide Level elevation with star showing salient behind the breakwater with the offset in elevation. 2023 surveys denoted by red (April), blue (May), yellow (November), and light blue (December).

DISCUSSION

Wave height reduction

The measured wave height reduction behind the breakwater was compared to empirical estimations of diffraction and transmission to determine which mechanism was dominant. Of the two, only transmission is expected to be influenced by the difference in crest height. If diffraction was the only important mechanism, the two inshore sensors should have measured roughly the same wave height reduction assuming the waves were shore normal and the gauges were placed consistently.

Diffraction

Diffraction diagrams appearing in the Shore Protection Manual (CERC 1984) were used to determine a diffraction coefficient (assuming shore normal waves) and ultimately a diffracted wave height for comparison to the measured data. At Graveling Point, wind waves make up the majority of the record. This correlates to a spreading value, Smax, of 10 (CERC 1984). Since the median offshore peak period was 2 seconds, the deep-water wavelength would have been 6.2 m according to linear wave theory. The median offshore depth at the gap was assumed to be the same as that measured at the offshore sensor which was 1.2 m. Using these values, the predicted diffraction coefficient at each inshore wave gauge was roughly 0.4. The diffraction predicted inshore wave heights are plotted against the measured inshore wave heights in Figure 14. The measured and calculated data line up well (1:1 line in the figure) behind the taller portion of the breakwater with a mean error of 0.8 cm. However, behind the shorter section only the smaller predicted/calculated wave heights agree. When offshore wave heights were greater than 0.15 m, diffraction alone appears to underestimate the wave height behind the shorter breakwater segment with a mean error of 4 cm. Whereas, diffraction for the taller portion overpredicts the inshore wave height by a mean error of only 2 cm for the same data range. This difference in mean error compared to the offshore wave height range of 0.15 m-0.3 m, represents an underprediction for the inshore wave height behind the shorter segment by 13%-27%, suggesting that there is an additional source of wave energy contributing to the inshore wave heights.

Transmission

The measured wave transmission was compared with two commonly used empirical formulas. The focus was placed on the large wave events (offshore>0.15 m). Figure 15 shows the comparison between the measured transmission coefficient data and that predicted by Briganti *et al.* (2003). The Briganti *et al.* equation predicts limited transmission across both the shorter and taller sides of the structure

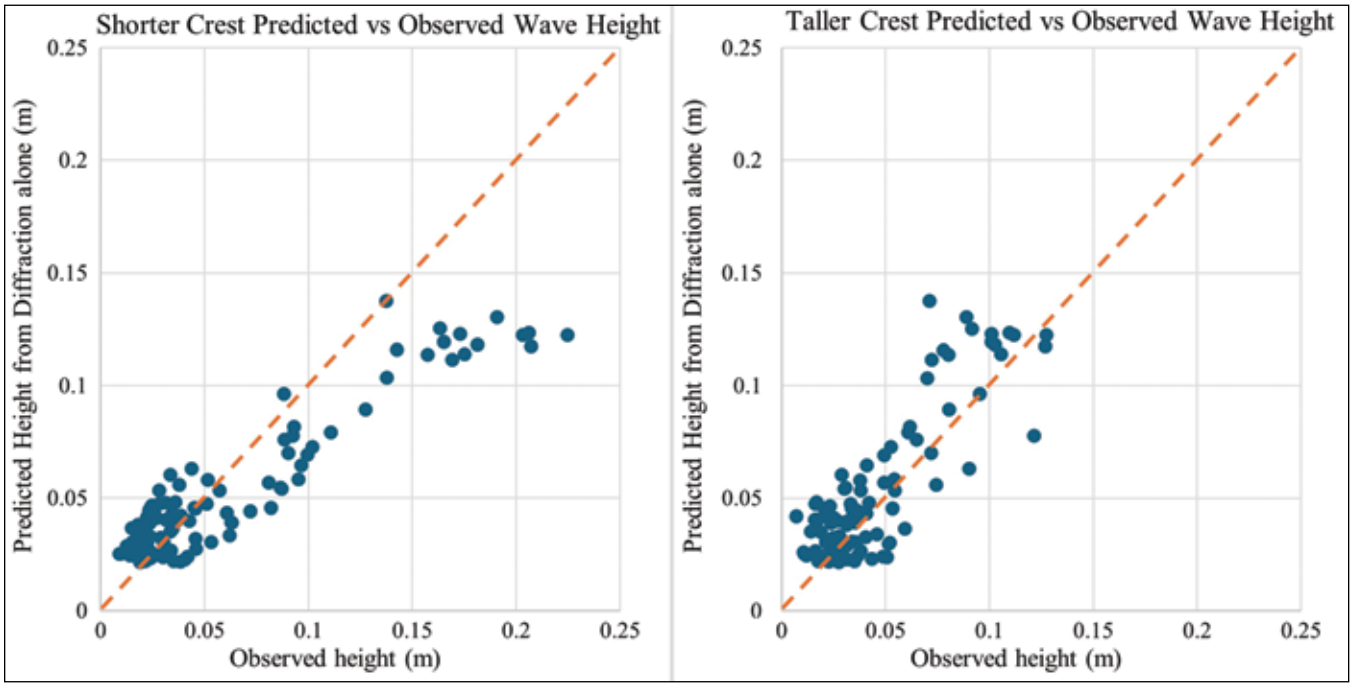

Figure 14. Predicted wave height from diffraction vs observed wave height (m).

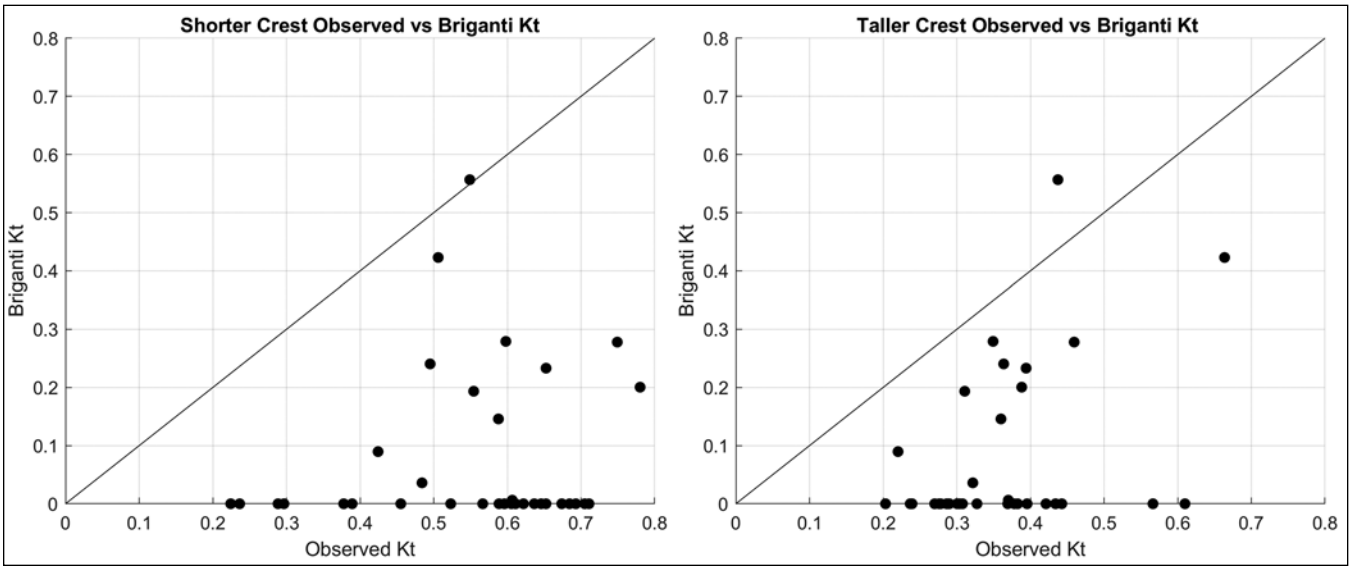

Figure 15. Briganti *et al.* (2003) K_t predictions compared to observed K_t for offshore waves taller than 0.15 m.

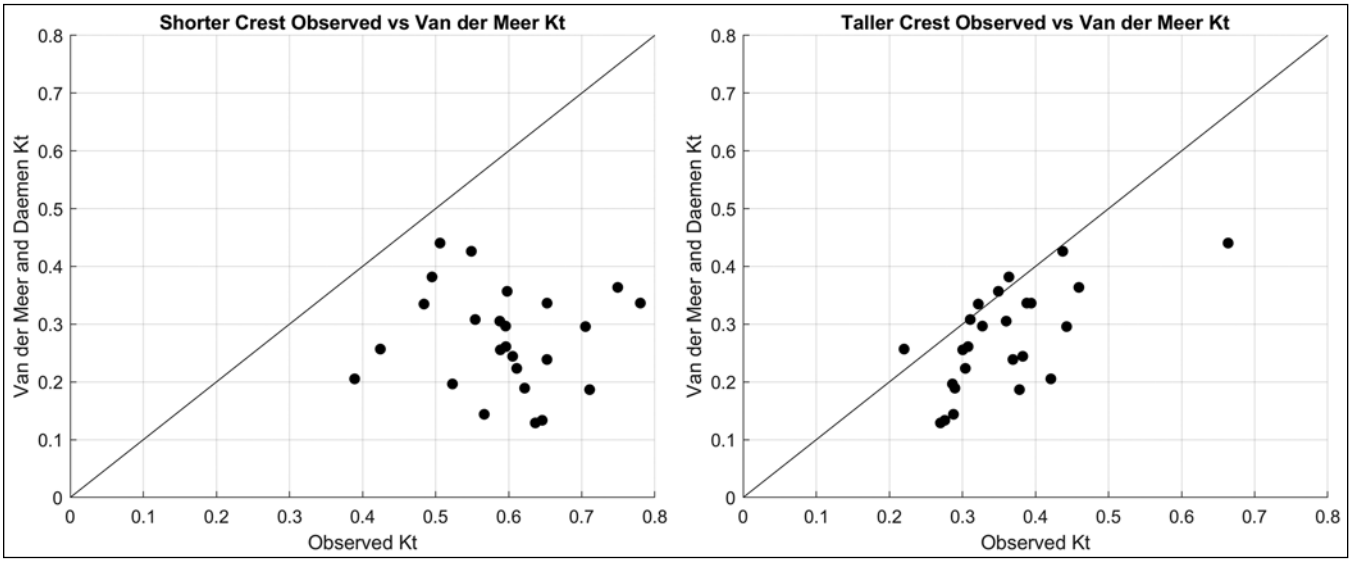

Figure 16. Van der Meer and Daemen (1994) K_t predictions compared to observed K_t for offshore waves taller than 0.15 m.

and nearly always underpredicts the observed transmission. When transmission is predicted to occur, the amount is similar for both the short and tall sections, with K_t values mostly ranging between 0.1 and 0.3, while the observed values routinely exceed 0.5. Figure 16 shows the comparison between the measured transmission coefficient data and that predicted by Van der Meer and Daemen (1994). Overall, the Van der Meer and Daemen equation predicts slightly higher transmission coefficients than Briganti *et al.*; however, in most cases, the predicted values are still significantly less than those measured. The fact that two commonly used wave transmission formulas consistently underpredict the amount of wave transmission suggests other processes may be important. The observed data also aligns well with the empirically tested wave transmission parameter ranges with the exception of the relative freeboard using D_{50} for Van der Meer and Daemen (Table 6). The relative freeboard observed was in the range of 0-1 instead of the empirically tested range of 1-6 since incident wave heights were small in comparison to the D_{50}.

Combined diffraction and transmission

While diffraction alone was able to adequately represent the observed wave heights behind the taller section of the breakwater, neither diffraction nor transmission alone were able to predict the observed wave heights behind the shorter section. One potential explanation is that during larger wave events, the wave height measured by the inshore gauge contains both transmitted and diffracted wave energy. To test this hypothesis, the wave height predicted by diffraction was simply added to that predicted by the two transmission formulas

Table 5.

Summary of GIS measurements of salient length and distance offshore.

	Salient length (m)		Distance offshore (m)	
Breakwater	Average	Range	Average	Range
A (east)	3.7	3.3-4.1	32.0	30.8-33.3
B	3.7	3.3-4.1	33.2	32.7-34.0
C	2.5	2.0-2.9	34.7	34.0-36.4
D (west)	2.4	1.7-3.0	41.0	39.8-43.7

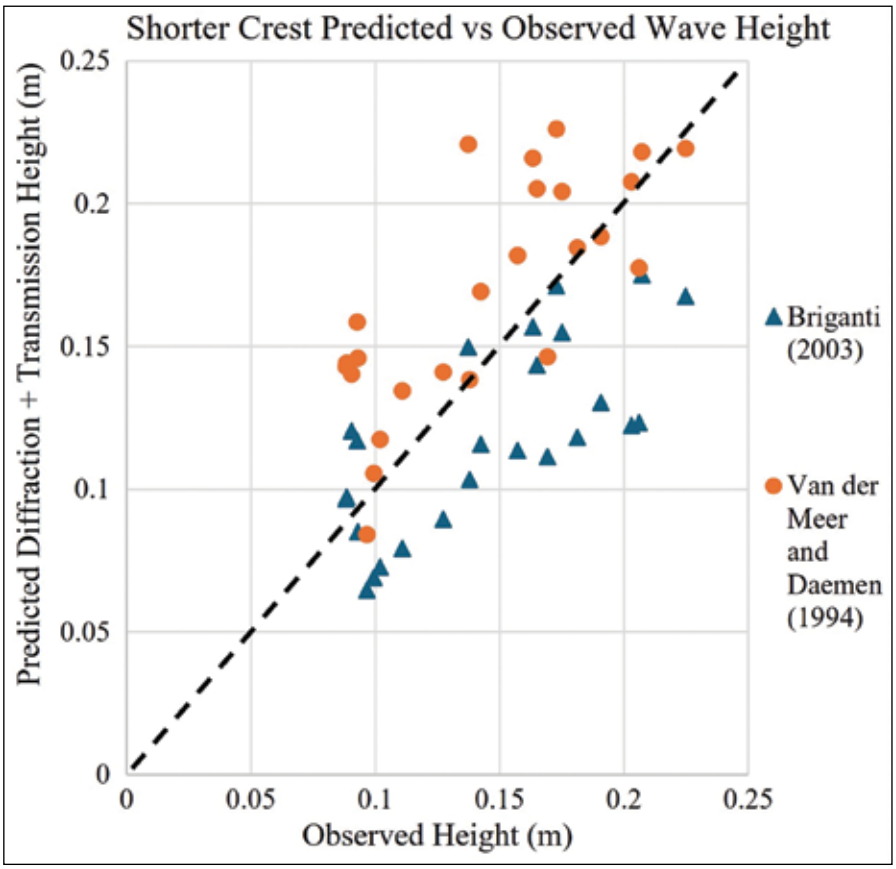

Figure 17. Shorter Crest predicted inshore wave heights from diffraction and transmission vs. the observed inshore wave height for offshore waves taller than 0.15 m.

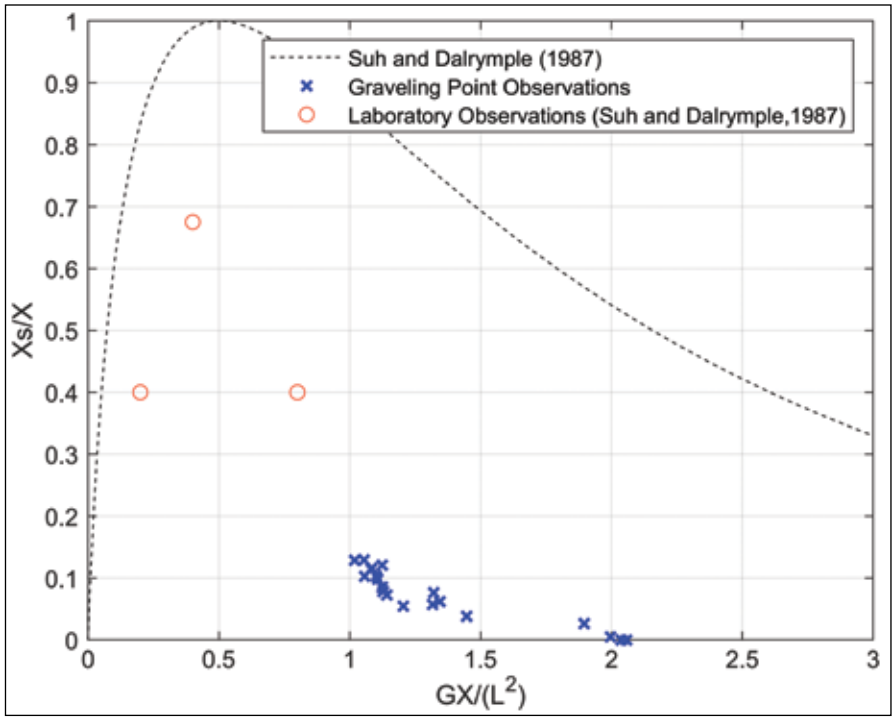

Figure 18. Modified from Suh and Dalrymple (1987) to include Graveling Point data.

and compared to the measured values. The result is shown in Figure 17, where the data points collapse around a 1:1 line indicating good agreement when using either transmission prediction added to the total diffraction. Van der Meer and Daemen (1994) slightly overpredict the inshore wave height by a mean error of 2 cm while Briganti *et al.* (2003) slightly underpredict the inshore wave height by a mean error of 2 cm. This is improved from an underestimated inshore wave height by a mean error of 4 cm.

In order to confirm these preliminary results, a longer study is recommended such that a wider range of wave conditions can be observed. In particular, it would be interesting to identify the parameters critical for separating the diffraction-dominated, transmission-dominated, and transmission/diffraction-dominated regimes.

The wave observations are based on two simplifying assumptions. First, the diffracted wave height is calculated assuming normally incident waves to the structure. This assumption is necessary due to the collection of non-directional wave data at the site. However, the influence of this assumption is thought to be minimal for the larger wave events of interest as the direction of the maximum fetch is aligned approximately shore normal to the structures (Figure 1). The second assumption is the phase-averaged diffracted and transmitted wave heights are combined through superposition. That is to say, the wave heights are combined without consideration for any phase effects.

Given these assumptions, it is impossible to assess which wave transmission equation better fits the observed data. Instead, the conclusion drawn is that small changes in crest freeboard can alter the relative importance of transmission and diffraction sources on the inshore wave height. The 10 cm difference in crest height between breakwaters is modest when compared to expected water level fluctuations associated with tides, storm surges and sea level rise suggest even modest levels of settlement may alter the relative contribution of transmitted wave height.

Shoreline response

Suh and Dalrymple (1987) developed an empirical equation to describe the influence of the non-dimensionalized breakwater geometry on shoreline response (Equation 6). A non-dimensional parameter characterizing the breakwater geometry (Equation 7) and two fit coefficients (C_1 and C_2) are used to predict the salient length (X_s).

$$Xs = X^{*}C_1\,(GX/L^2)\,e\,(C_2\sqrt{\{GX/L^2\}}) \quad (6)$$

$$GX/L^2 \quad (7)$$

Suh and Dalrymple fit the equation to field observations collected by others. The determined coefficients are presented in the second column of Table 7. In addition, Suh & Dalrymple conducted three laboratory tests with varied breakwater geometries to study the influence of gap length. Figure 18 depicts the non-dimensionalized shoreline response as a function of the breakwater geometry (Equation 7) including the laboratory data collected by Suh & Dalrymple. There is relatively poor agreement between the laboratory data and the curve determined by Suh and Dalrymple (Figure 18). They noted the laboratory tests had similar slopes and Dean numbers to the field observations. The Dean number relates breaking wave height and period to sediment fall velocity which can be used to characterize the expected beach profile (Dean 1973). Therefore, they proposed the difference between the field data and laboratory response was likely due to varied wave climate.

Interestingly, the laboratory data collected by Suh and Dalrymple and the field observations from Graveling Point are relatively consistent. The median offshore peak period for Graveling Point was 2 sec whereas the laboratory models used a period of 1.2 sec. The median offshore wave height for Graveling Point was also only about 9 cm whereas the laboratory models had a deepwater wave height of 3.51 cm and breaking wave height of 3.20 cm.

The Graveling Point data and Suh and Dalrymple laboratory data appear to have a consistent shape with the original curve, however with a vertical shift in the amplitude of the shoreline response (Figure 19). It is hypothesized that this damped shoreline response is likely due to the lower wave energies of both the Graveling Point and laboratory data.

To test the original expression to characterize the low-energy sites, modified coefficients of the Suh and Dalrymple equation to fit the Graveling Point and laboratory data are proposed. Two cases are considered. Case 1 includes only the Graveling Point data whereas Case 2 includes both the Graveling Point data and laboratory data from Suh and Dalrymple. In both cases, the coefficients (C_1 and C_2) are determined by minimizing the root mean squared error (RMSE) with the constraint that the non-dimensional salient amplitude cannot exceed 1 (i.e., tombolo). The results are shown in Table 7 and Figure 19.

Table 6.

Comparing limitations of wave transmission formulas listed in Hassanpour *et al.* (2023) to range observed at Graveling Point (see Equation 4 and Equation 5) ✓= observed data at Graveling Point within acceptable ranges, N/A= no observed data within accepted range, X= observed data outside acceptable range.

		<= -2.5	<= 0	<= 2.5	<= 5	> 5
Briganti	R_c/H_i	N/A	✓	✓	✓	
Van der Meer and Daemen	R_c/D_{50}		✓	✓		
Briganti	S_{op}			✓		
Van der Meer and Daemen	S_{op}			✓		
Briganti	B/H_i			N/A	✓	✓
Van der Meer and Daemen	H_i/D_{50}			X	N/A	N/A

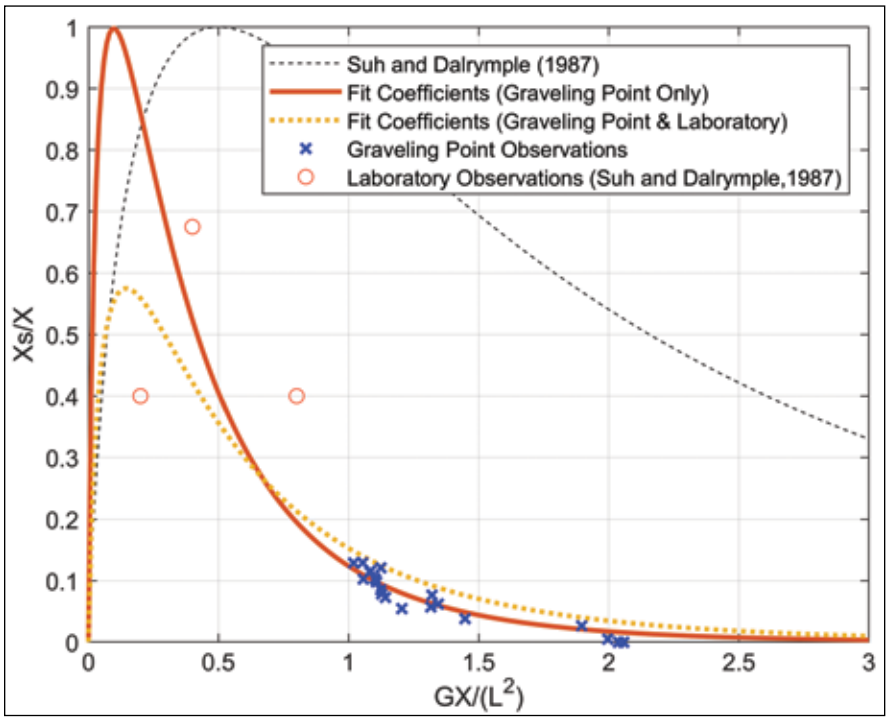

Figure 19. Adjusted coefficients of Suh and Dalrymple (1987) to better represent present study.

Both curves show relatively good agreement for the limited range of geometries present at Graveling Point. RMSE values range from roughly 8% to 2% (in non-dimensionalized salient amplitude). Due to the limited range of geometries, the robustness of the proposed coefficients is low. There is considerable variation in the predicted shoreline response between Case 1 and Case 2 for the geometries expected to have the greatest shoreline response (i.e., near 0.5). More observations are needed to predict when (or even if) a tombolo would form for sites with low-energy wave climates similar to Graveling Point. However, in the short term, it is suggested that application of the original equation be done with an understanding that the

Table 7.

Fit coefficients for original and modified Suh and Dalrymple (1987) equation.

	Suh and Dalrymple (1987)	Graveling Point	Graveling Point & Suh and Dalrymple lab data
C1 (Power Term)	14.8	76.0	29.4
C2 (Exponential Decay Term)	-2.83	-6.42	-5.26
RMSE	N/A	0.014	0.078

shoreline response will likely be damped at low-energy sites.

CONCLUSIONS

The recently constructed living shoreline project at Graveling Point presented a unique opportunity to study the impact of crest height on wave transmission and resulting shoreline evolution. One of the breakwaters has a noticeable 10 cm difference in crest height from one half to the other. The original hypothesis was that wave transmission would be noticeably higher across the shorter section and that the salient would be deflected towards the taller crest portion of the structure. Over a one-month period of wave observation, field measurements revealed only a small difference in measured transmission across the tall (K_t=0.36) and short (K_t=0.41) sides of the breakwater. However, during larger wave events (offshore>0.15 m) the difference is more significant (tall K_t= 0.35, short K_t=0.60). When comparing the measured transmission to two common empirical formulas, the formulas underpredict the amount of transmission suggesting another mechanism for transferring energy to the lee side of the structure. The most obvious mechanism is wave diffraction through the gaps. Diffraction diagrams from the Shore Protection Manual (CERC 1984) were used to calculate diffracted wave heights at the inshore location. The diffracted wave heights match the observed wave heights well behind the higher crest portion of the breakwater, but underpredict the wave height behind the shorter section. This suggests that while diffraction is dominant behind the taller section of the breakwater, the wave heights behind the shorter section are likely due to the contribution of both the diffracted and the transmitted wave over the breakwater. To test this theory, the diffracted wave heights were added to those predicted by both the Briganti *et al.* (2003) and Van der Meer and Daemen (1994) wave transmission equations and compared to the observed wave heights. The resulting fit was improved from an underestimated observed inshore wave height with a mean error of 4 cm to an overprediction mean error of 2 cm by Van der Meer and Daemen (1994) and an underprediction mean error of 2 cm by Briganti *et al.* (2003). The reduced mean error suggests that the combination of diffracted and transmitted wave energy is responsible for the inshore wave heights behind the shorter breakwater segment.

While it is recognized that the data set collected represents only a small range of possible conditions at the site, the observations suggest that both wave transmission and diffraction play an important role in determining inshore wave heights. Specifically, as wave transmission is related to freeboard, the relative importance of transmission and diffraction will change with water level fluctuations associated with tides, storms, and sea level rise.

The shoreline at Graveling Point responded near instantaneously. Salients were observed behind all four breakwaters in a morphological dataset collected two weeks after completion of the beach nourishment. The observed salient amplitude was lower than predicted using the widely cited Suh and Dalrymple (1987) equation, but as offshore distance varied with each breakwater and over time, the salients generally followed the expected pattern of decreasing in length with increased offshore distance (Table 5). It is thought this underprediction is related to the low-energy conditions at Graveling Point. The original expression generated by Suh and Dalrymple was refit using a combination of the Graveling Point field data and laboratory data from the original paper with wave conditions similar to those observed in the field at Graveling Point.

The result is a set of coefficients for a low-energy version of the Suh and Dalrymple curve that provided reasonably good agreement (RMSE of 8%) over the limited range of non-dimensionalized breakwater configurations present at the site. This suggests the original non-dimensional relationships relating breakwater length, gap and distance offshore as proposed by Suh and Dalrymple are efficient means to estimate salient amplitude with low-energy scaling effects captured by fit coefficients. In order to affirm the robustness of the new curve, additional field data needs to be collected at low-energy sites. However, in the short term, it is suggested that application of the original equation be done with an understanding that the shoreline response will likely be damped at low-energy sites.

ACKNOWLEDGEMENTS

This work was performed with funding through the Coastal Protection Technical Assistance Service from the New Jersey Department of Environmental Protection. The authors gratefully acknowledge the faculty, staff, and students of the Coastal Engineering Research Group at Davidson Laboratory, Stevens Institute of Technology, who contributed to field data collection. The authors also acknowledge T&M Associates for sharing the design plans.

REFERENCES

Briganti, R., Van Der Meer, J., Buccino, M., and M. Calabrese, 2003. "Wave transmission behind low-crested structures." *Proc. Coastal Structures 2003*, 580-592. DOI: http://dx.doi.org/10.1061/40733(147)48.

Chasten, M.A., Rosati, J.D., and J.W. McCormick, 1993. "Engineering design guidance for detached breakwaters as shoreline stabilization structures." Technical Report CERC-93-19. USACE, Vicksburg, MS. https://hdl.handle.net/11681/12542.

Coastal Engineering Research Center. 1984. "Shore Protection Manual, Vol. I." CERC, Dept. of the Army, U.S. Army Corps of Engineers, Washington, DC. https://usace.contentdm.oclc.org/digital/collection/p16021coll11/id/1934/.

d'Angremond, K., Van Der Meer, J.W., and R.J. De Jong, 1997. "Wave transmission at low-crested structures." *Proc. Coastal Engineering 1996*, 2418-2427. DOI: 10.1061/9780784402429.187.

Dally, W.R., and J. Pope, 1986. "Detached breakwaters for shore protection." Technical Report CERC-86-1. USACE, Washington, DC. https://apps.dtic.mil/sti/citations/ADA171183

Dean, R.G., 1972. "Heuristic Models of Sand Transport in the Surf Zone." *Proc. Engineering Dynamics in the Surf Zone*, 208-214. https://search.informit.org/doi/10.3316/

Hassanpour, N., Vicinanza, D., and P. Contestabile, 2023. "Determining wave transmission over rubble-mound breakwaters: Assessment of existing formulae and benchmark testing." *Water,* 15(6), 1111. DOI: 10.3390/w15061111.

Karimpour, A., Chen, Q. 2017. "Wind wave analysis in depth limited water using OCEANLYZ, a MATLAB toolbox." *Computers & Geosciences*, 106, 181-189. DOI: 10.1016/j.cageo.2017.06.010

Kerr, L., Zuck, N., and J.K. Miller, 2020. "Wave analysis for Mystic and Parkertown beaches, Little Egg Harbor Township." SIT-DL-20-9-CV2, Stevens Institute of Technology, Davidson Laboratory, Hoboken, NJ.

Suh, K., and R.A. Dalrymple, 1987. "Offshore breakwaters in laboratory and field." *J. Waterway, Port, Coastal and Ocean Engineering,* 113(2), 105-121. https://doi.org/10.1061/(ASCE)0733-950X(1987)113:2(105).

U.S. Army Corps of Engineers Philadelphia District, 2021. "Public Notice." CENAP-OPR-2021-00067-97.

Van der Meer, J.W., and I.F. Daemen, 1994. "Stability and wave transmission at low-crested rubble-mound structures." *J. Waterway, Port, Coastal, and Ocean Engineering,* 120(1), 1-19. DOI: 10.1061/(ASCE)0733-950X(1994)120:1(1)

Zimmerman, T., Jansen, K., and J. Miller, 2020. "Analysis of UAS flight altitude and ground control point parameters on DEM accuracy along a complex, developed coastline." *Remote Sensing,*12(14), 2305. DOI: 10.3390/rs12142305.